

Influence of atmospheric circulation types in space - time distribution of intense rainfall

Nikos Mamassis and Demetris Koutsoyiannis

Department of Water Resources, Faculty of Civil Engineering, National Technical University, Athens, Greece

Abstract. The influence of the prevailing weather situation on the temporal evolution and geographical distribution of intense rainfall is studied, as a potential tool to improve rainfall prediction. A classification scheme of the atmospheric circulation over the east Mediterranean territory is used for the analysis. The study area is the Sterea Hellas region (central Greece) with an area of about 25,000 km². Daily data from 71 rain gages and hourly data from three rain recorders over a 20 year period are used. From these data sets, the intense rainfall events were extracted and analyzed. Several empirical and statistical methods (also including the available tools of a Geographical Information System) are used for the analysis and comparison of rainfall distribution both in time and in space. The analysis shows that the contribution of the concept of weather types to the quantitative point rainfall prediction in short timescale is small, and only the estimation of the probability of occurrence of an intense event is feasible. On the contrary, the relation between the spatial distribution of rainfall and the atmospheric circulation patterns is significant and may be used for improving the forecasting of the geographical distribution of rainfall.

1. Introduction

The space-time evolution of the rainfall process is related to the characteristics of the prevailing weather situation that caused the rainfall. To study more effectively this relationship, several researchers have classified similar weather situations of particular regions into specific types. The classification schemes generally fall into three main categories, each corresponding to a different approach to the compilation of the meteorological data and weather maps.

The first category includes the schemes that are based on the combination of the different value ranges of several local meteorological variables. *McCabe* [1989] separated the range of wind direction into three classes and the range of cloudiness values into two classes. Combining these classes, he defined six weather types, which were used by *Hay et al.* [1991] for the classification, modeling, and simulation of daily rainfall in a watershed in the United States. *Wilson et al.* [1991] used surface air pressure and 850-hPa level temperature to classify and simulate daily rainfall in the northern Pacific. *McCabe* [1994] used height anomalies (in meters) for the 700-hPa level, to represent atmospheric circulation of the western United States, and relate that to the variability of the snow-pack accumulation. *Hughes and Guttorp* [1994] used sea level pressure to classify several weather states and to relate them to daily rainfall in the state of Washington.

The second category includes the classification schemes related to the meteorological feature that generated the rainfall, such as a front passage (cold, warm, occluded), a thermal instability or another local meteorological phenomenon. *Shaw* [1962] in England and *Huff* [1969] in the United States used this type of classification for the study of daily rainfall.

The third category includes the classification schemes related to the atmospheric circulation over a specific territory. These schemes are based on large-scale features of the general atmospheric circulation such as the location of pressure centers, the cyclone trajectories, or some special air pressure distributions in several levels of the atmosphere. *Baur et al.* [1944] introduced a weather classification scheme of the mean

air pressure over a wide area larger than Europe. This scheme was based on a timescale of several days (at least three) considering that the main features of weather across Europe remain constant during one time step of that length. *Bardossy and Plate* [1991, 1992] used this scheme for daily rainfall modeling and simulation in Germany. Following the scheme of *Baur et al.* [1944], *Duckstein et al.* [1993] developed a circulation pattern classification scheme for the continental United States and used it to relate flood occurrence in central Arizona to circulation patterns. *Schuepp* [1968] developed a weather classification scheme for the European Alpine region, based on the air mass advection (related to source areas), temperature characteristics, and cyclonicity. This scheme was used for the study of daily runoff in northern Italy by *Van de Gried and Seyhan* [1984]. *Lamb* [1950, 1972] defined a classification scheme of atmospheric circulation for the British Isles, based on the specific patterns in weather maps of the surface and the 500-hPa level. *Wilby* [1994] used *Lamb's* scheme to simulate circulation patterns and hence daily rainfall in England and *Wilby et al.* [1994] to simulate daily flows. *Wilby* [1995] used the same scheme to study and model daily rainfall in England by incorporating also in the classification the presence or absence of weather fronts. *Maheras* [1982], based on the *Lamb* [1972] method, introduced a classification scheme of atmospheric circulation over the East Mediterranean territory. This scheme was used by *Mamassis and Koutsoyiannis* [1993] and *Mamassis et al.* [1994] for the analysis of intense rainfall and flood events in Greece and was also adopted in this study. Details of this classification scheme are given in section 3.

Weather classifications may be viewed as a systematization of meteorological experience in a particular region. Obviously, there is a relationship between the geographical characteristics of a particular area (such as the geographical location, the relative position with regard to the sea, the orography), and the climatological regime in this area. This relation may be captured empirically by using weather types and studying their influence on hydrometeorological processes. This approach can potentially be combined in a complementary way with the outputs of general circulation models (GCM) in order to downscale these outputs to a finer spatial scale, localized to the specific area of interest. In particular, the empirical study of the relationship between weather types and the rainfall process in a specific area may be useful to translate the synoptic conditions used to define the weather types, into quantitative information about rainfall. If such a relationship can indeed be established, it will improve rainfall prediction on a local scale. With regard to these aspects, research was recently carried out [*Wilson et al.*, 1991; *Bardossy and Plate*, 1992; *Hay et al.*, 1991; *Hughes and Guttorp*, 1994; *Wilby*, 1994, 1995], especially in the modeling and simulation of daily rainfall in specific areas utilizing the local meteorological experience.

This paper contributes to the study of the influence of weather types on (1) the temporal evolution of point rainfall and the stochastic structure of intense rainfall events, and (2) the geographical (spatial) distribution of intense rainfall. For the first issue we examine the rainfall process at a fine timescale, from hourly to daily, as well as the total storm characteristics of intense rainfall events (such as the duration and total depth). To the authors' knowledge no previous similar study has been carried out at an hourly timescale. For the second issue related to the spatial distribution of daily rainfall, we use a Geographical Information System (GIS) to construct

daily rainfall fields and process them statistically. Similar studies have typically used multivariate models for that purpose.

This paper is outlined as follows: In section 2 the study area and the available data sets are described and in section 3 the weather type classification scheme is presented. In section 4 the point rainfall process on an hourly basis as well as the total storm characteristics of intense rainfall events are studied. In section 5 the methodology of analyzing the spatial distribution of rainfall using a grid-based technique is described. Finally, the conclusions are presented in section 6.

2. Study Area and Data Used

The study area is the Sterea Hellas region (central Greece) with an area of approximately 25,000 km² (about one fifth of the total area of Greece, Figure 1). This region includes five important and many smaller rivers. One of them (the Acheloos River) is the largest river (in discharge) in Greece providing water for irrigation and hydropower. Three others (Evinos, Mornos, B. Kifissos) provide water supply to the area of Athens. The Pindus mountain chain on the west side of this region causes heavy orographic rainfall and therefore a wetter rainfall regime, as compared to that of the east side. Thus the annual rainfall varies from about 2000 mm in the north-western part of the region to about 400 mm in the southeastern part (Athens).

Daily rainfall data from 71 rain gages over the entire region and hourly rainfall data from three of them equipped with rain recorders (Krikello, Aniada, Drymonas, located at the Evinos River basin) were available for a 20 year period (1970-1990). Figure 1 shows the general location of the study area, its morphology, and the available rain gages.

From the continuous records we have extracted and studied only the intense rainfall events. Intense rainfall has the most practical interest as it is responsible for extreme floods in the study area. From the hourly point rainfall data sets the intense rainfall events were extracted using a criterion based on a threshold of hourly rainfall (above 7 mm) or daily rainfall (above 25 mm). Analysis was performed on the data of all the three rain-recording stations mentioned above, but here we present the results from one of them (Krikello), as those of the other stations were very similar. The intense rainfall events were separated into rainy (October to April) and dry (May to September) season events. In total, 200 events belong to the rainy and 93 events to the dry season.

For the daily data sets of the 71 gages the intense rainfall days were extracted using a criterion based on a threshold of daily point rainfall (above 80 mm) in any one of them. Again, the intense rainfall days were separated into rainy and dry season with 316 and 31 intense rainfall days, respectively, in each season.

3. Weather Type Classification Scheme

The intense rainfall events and days were classified according to the prevailing weather situation, using a daily calendar of synoptic weather types in Greece (P. Maheras, unpublished calendar, 1991). As we mentioned in the introduction, we used the classification scheme introduced by Maheras [1982], based on the atmospheric circulation over the eastern Mediterranean. The main features of the atmospheric circulation considered for the classification were (1) the positions of the

Figure 1

centers of the anticyclones, (2) the main trajectories of the cyclones, and (3) some special synoptic situations at the surface and at the 500-hPa level.

According to this scheme the circulation patterns of the territory were classified into five anticyclonic, six cyclonic, two mixed, and three characteristic weather types [Maheras, 1982]. Table 1 shows a summary description of the above weather types. Figure 2 shows the main trajectories of the six cyclonic weather types which are responsible for bad weather and produce the main amount of rainfall in the study area. In four of them (W1, SW1, NW1, W2) the disturbance passes near the study area and provokes intense rainfalls, especially on the west side of the area where the Pindus mountain chain lies. The SW1 and NW1 weather types are very common in Greece especially in the rainy season and have a significant influence on the annual rainfall regime of the study area. In the other two cyclonic types the disturbance passes a long distance away from the study area and the generation of intense rainfall is rare. Especially for the SW2 weather type, the trajectory of the cyclone passes through the Aegean Sea and is often responsible for intense rainfall on the eastern side of the study area.

Figure 3 shows a weather map of the 500-hPa level corresponding to the weather type DOR. The presence of a cold air mass at this level above Greece combined with a field of low pressures with a weak gradient on the surface is typical for this weather type. This weather situation has a high frequency of occurrence in the dry season and causes atmospheric instability and intense convective rainfall at several sites in Greece without a typical areal distribution.

4. Influence of Weather Types to Point Rainfall

In this section we use statistical methods to detect whether the prevailing weather type affects the point rainfall characteristics or not. More specifically, we examine the probability of occurrence of intense rainfall, the total duration and depth, and the hourly point rainfall structure and compare statistically these characteristics among different weather types.

The conditional probability of occurrence of an intense rainfall event, given the prevailing weather type, was calculated using the Krikello data set and the daily calendar of weather types. Table 2 shows this probability for each weather type and Figure 4 for grouped weather types. To examine if there are statistically significant differences in probabilities (proportions of rainy days to the total number of days) among weather types, we have applied the proportion statistical test [Freund and Simon, 1991, pp. 386-388]. The analysis shows that there are statistically significant differences (at all typical significant levels down to 1%) among the four groups of weather types for both the rainy and the dry season.

For each intense rainfall event we extracted the duration, total depth, and mean intensity. Their sample characteristics (median, maximum and minimum value, and upper and lower quartile) for the most frequent weather types are shown in the box plots of Figure 5. The statistical analysis showed that in some cases there are statistically significant differences among the characteristics of different weather types. More specifically, in the rainy season the types SW2, NW2 exhibit statistically significant differences in the rain duration from the other types (at a 5% significance level), whereas the W2 type exhibits significant differences in the total depth and mean intensity from the other types (at a 1% significance level). In

Table 1

Figure 2

Figure 3

Table 2

Figure 4

Figure 5

the dry season the differences in the duration and total depth among the various weather types are statistically significant (at a 1% significance level) almost in all cases. However, in a more quantitative point of view these differences are not so important, as they explain a small percentage of variance of these characteristics. Specifically, as shown in Table 4, the percentage of variance explained by weather types for the various characteristics varies from 3% to 7% for the rainy season and from 8% to 18% for the dry season.

Furthermore, we have calculated the marginal statistics (mean and standard deviation), as well as the autocorrelation function of hourly depths, which are shown in Table 3 for the different weather types. No statistically significant differences in the hourly depth are detected among different weather types. Hence only 1% of the variance of the hourly depth is explained by the weather type concept for the rainy season and 2% for the dry season (Table 4). Finally, there are no statistically significant differences on the autocorrelation function of hourly depths among weather types, but there are differences between the two seasons (Table 3). The atmospheric instability which characterizes the rainy days of the dry season explains the strong variability of rainfall which leads to a weaker autocorrelation function of hourly depth on this season.

Table 3

Table 4

5. Influence of Weather Types to the Geographic Distribution of Rainfall

In this section we examine the geographical distribution of rainfall on a daily basis using a grid-based approach. The daily data values were stored and analyzed using a GIS. For each intense rainfall day the measured values of point rainfall were used to determine a representative precipitation depth at all grid cells of the study area. The algorithm used consists of the following steps [Dingman, 1994]: (1) A grid covering the study area is established. The grid spacing depends on the analyst but is usually about one tenth of the average distance between rain gages. In this study, the average distance between the rain gages was about 19 km and thus the grid spacing was chosen as 2 km. (2) Values of precipitation at each grid cell are estimated as linear combinations of the measured values, that is,

$$p_i = \sum_{g=1}^G w_{ig} * p_g \quad (1)$$

where p_i is the estimated precipitation at the i th grid cell, p_g is the measured precipitation at station g , and w_{ig} is the weight assigned to station g for cell i .

Several methods can be used to estimate the weights w_{ig} , such as the isohyetal, least squares, polynomial, spline, inverse distance weighted (IDW), and kriging methods [Dingman, 1994]. Some of these methods (isohyetal, least squares) are not appropriate for our purpose, because they derive surfaces that do not preserve the measured point values exactly. A comparison of mean annual and monthly rainfall surfaces, calculated using several of the above and other methods (Thiessen, cokriging), has been done for the study area [Joulis, 1996]. The analysis showed that both the IDW and the kriging methods resulted in similar rainfall spatial distributions and about the same total areal rainfall depth (the differences were about 1-2 %). Also, the areal rainfall depth did not depart significantly from that estimated by the tradi-

tional Thiessen method. In this study the IDW method, which combines simplicity, availability in the GIS, and preservation of the measured point values, was selected for estimating the weights w_{ig} . Another advantage of the IDW method is that it does not require the rainfall field to be spatially homogeneous, as it simply performs a local linear estimation. This feature is very important in our case, where there exist apparent spatial inhomogeneities in the rainfall characteristics over the study area. On the contrary, the kriging method typically makes the assumption of a constant semivariogram over the entire area, which is not strictly valid in our case.

We remind that in the IDW method the weights w_{ig} are a function of the distance between each of the grid cells and each of the rain gage locations, given by

$$w_{ig} = \frac{d(i,g)^{-b}}{\sum_{s=1}^G d(i,s)^{-b}} \quad (2)$$

where $d(i, g)$ is the distance between the grid cell i and the gage g , G is the total number of gages, and b is a chosen parameter, usually assigned to 1 or 2. In the case where a grid cell is also a gage location, the rain depth assigned to this cell is the value measured by the gage and the weights for the other gages become zero.

The grid-based approach described above, which is based on the fitting of a surface to point data, has some advantages when compared to other methods, such as the multivariate analysis. For example, it does not require filling of missing data in order to fit a surface and offers a better understanding and visualization of the rainfall field (e.g., localization of regions with specific characteristics). Also, the approach allows for the calculation of statistical surfaces instead of point statistics, as described later in this section. The rainfall surfaces can be combined with geographical, geological, and land use surfaces for rainfall-runoff modeling. An apparent weakness of the approach is that in most grid cells the rainfall values are estimates rather than measurements, which obviously introduces errors in the field representation.

The analysis was performed only for the rainy season due to the small number of intense rainfall days in the dry season. Several methods were used for the analysis and comparison of the rainfall spatial distribution.

As a first step, the rainfall fields in each weather type were plotted using an appropriate color or gray scale, thus visualizing the spatial rainfall distribution. This assists the localization of areas attracting intense rainfall. Then, the statistical surfaces (mean, standard deviation, coefficient of variation) of the daily rainfall were calculated for each weather type. In these statistical surfaces, each cell takes the value of the statistic (mean, standard deviation, coefficient of variation) of the corresponding cells of daily rainfall surfaces over each weather type.

The statistical surfaces of each weather type are shown in Figure 6, indicating that the geographical distribution of rainfall in the study area is strongly affected by the weather type. In cyclonic types the spatial distribution of rainfall is related to the trajectory of the disturbance. The W1, W2, SW1 types provoke intense orographic rainfall in the western areas where the Pindus mountain chain lies. As indicated from the statistical surfaces, the intense rainfall almost always occurs in this specific area. The NW1 and NW2 types provoke rainfall in the same area but with larger spatial variability. The SW2 type

Figure 6

provokes intense rainfall in the eastern side of the study area. In mixed types the combination of an anticyclone over Europe and a cyclone over the Aegean Sea (Table 1) provokes bad weather and rainfall in the eastern part of our study area, and especially in the northern Evia. In the remaining types, including all the anticyclonic and dry types, the few intense rainfall events are related to the local atmospheric instability, and hence no typical spatial distribution appears.

Furthermore, the correlation coefficients among all the rainfall surfaces of the same weather type were calculated, and their empirical distribution function was studied. Figure 7 shows the sample characteristics (median, maximum and minimum value, and upper and lower quartile) of correlation coefficients for each weather type. The majority of the correlation coefficients are positive for all weather types. That means that different intense rainfall events of the same weather type are positively correlated in space. This indicates a similarity in the spatial distribution of different rainfall events belonging to the same weather type. Notably, as shown in Figure 7, all correlation coefficients of the events of the W1 type are positive, and most of the others have their lower quartile positive. There are two exceptions, related to the types NW1 and SW2, whose lower quartiles are negative and ranges of the correlation coefficients are wider, thus indicating larger spatial variability of rainfall. Yet, the median remains significantly higher than zero for both types. In addition, as we observe in Figure 6, the rainfall produced by these two weather types is generally attracted at certain locations of the study area, as NW1 causes heavy rainfall in the western part and SW2 in the eastern part of the study area. For comparison we have plotted in Figure 7 (last box) a box plot of the sample correlation coefficients of all events, regardless of the prevailing weather type. We observe that in this case the range of the correlation coefficient covers almost all the feasible interval $[-1, 1]$. The positive median (0.15) reflects the inhomogeneity of the general rainfall regime in the study area, with higher rainfall in the Pindus mountain chain.

As another technique to quantify the influence of weather types on the rainfall distribution, apart from the grid-based analysis described above, we also performed an analysis based on the separation of the study area into subareas. Specifically, we have separated the study area into 10 subareas (Figure 1) climatically homogeneous, considering also the borders of hydrologic basins for the separation. The statistics of the areal rainfall of each subarea and each weather type were calculated. The mean daily rainfall per subarea and weather type is presented in Table 5. We observe in Table 5 that each weather type affects a number of neighboring subareas and each subarea is affected by specific weather types (for example, Evia is affected mainly by MT2 and SW2). To this latter rule there is the exception of the Sperchios subarea, which is equally affected by all weather types. Again we conclude from Table 5 that the cyclonic types W1, W2, NW1, and SW1 affect the western subareas and the SW2 and MT2 types affect the eastern subareas.

The Kruskal-Wallis statistical test [Freund and Simon, 1991, pp. 498-499] showed that there are statistically significant differences at a 1% significance level in the rainfall of a specific subarea among weather types, as well as in the rainfall produced by a specific weather type at various subareas. Table 6 shows the results of the analysis of variance of areal daily rainfall depth in the 10 subareas. The analysis of variance showed that a large percentage of the variance of the

Figure 7

Table 5

Table 6

rainfall depth (more than 20% in 7 out of 10 subareas) is explained by the concept of weather type. The values of the explained variance given in Table 6 are not negligible like those of hourly depth (Table 4). This may be interpreted as an indication that the influence of the weather type on rainfall depth increases with the increase of the timescale (from hourly in Table 4 to daily in Table 6). To get a more solid understanding of the influence of timescale to the percentage of variance explained by weather types, we aggregated the Krikello hourly point rainfall depths of the rainy season to 6-, 12-, and 24-hour timescales and we performed analysis of variance for each scale. The analysis showed that the percentage of explained variance has a very small increase with the increase of the timescale. Specifically, the percentages are 1.0%, 2.3%, 2.9%, and 3.9% for 1, 6, 12, and 24 hours, respectively.

Thus the increase of timescale does not explain much of the difference between the results of Table 4 and Table 6. Consequently, the major part of this difference is explained by the different criteria used for extracting the intense rainfall events in the two cases. In the first case (Table 4), the selection of events was based on the value of rainfall intensity or depth at a point location, whereas in the second case (Table 6), the selection was based on the magnitude of the rainfall depth at any point of the study area. The data set of the second case includes events that did not give rainfall at all at the point location of the first case (Krikello). It is anticipated that, if every event was considered, regardless of the rainfall magnitude (i.e., without a selection criterion), the percentage of variance explained by weather types would be even higher, as the anticyclonic types would have a larger participation in the sample. The apparent dissimilarities of anticyclonic and cyclonic weather types would affect further the results of analysis of variance. This is the case, for example, in the study of *Bardossy and Plate* [1991, 1992], where all events are considered and the connection between rainfall and circulation patterns is quite stronger.

6. Conclusions

In this study we have explored the connection between the structure of intense rainfall in space and time and the atmospheric circulation patterns in a large area in Greece. In the analyses performed, we have used records (in hourly through daily timescale) of intense rainfall events, in order to investigate whether weather types can contribute to the prediction of flood-producing storms.

The analysis of point rainfall characteristics shows that there are essential differences in the probability of occurrence of an intense rainfall event among weather types. On the other hand, the introduction of the concept of weather types has a very small contribution to the explanation of variability and structure of point rainfall.

The analysis of spatial distribution of rainfall in the study area, in connection to the weather types, shows that the prevailing weather type affects strongly the spatial rainfall fields. This conclusion is confirmed by the results of various analyses, such as the differences of statistical rainfall surfaces among different weather types, the strong correlation among the daily rainfall surfaces of the same weather type, and the analysis of variance of the areal daily rainfall in selected subareas. The results are consistent with the definition of

weather types and the physiographical characteristics of the study area.

Overall, the analysis shows that the contribution of the concept of weather types to the quantitative rainfall prediction in short timescales is small, but the estimation of the probability of occurrence of an intense event is feasible. On the contrary, the strong relation between the spatial distribution of rainfall and the atmospheric circulation patterns may be used for improving the forecast of the geographical distribution of rainfall.

Acknowledgments. A part of this study was performed under the framework of the research project AFORISM funded by the European Union, DG XII (EPOC-CT90-0023). We are grateful to P. Maheras for providing us with the daily calendar of weather types. We thank A. Kazakos for the English review. We appreciate the constructive comments by the Guest Editor E. Foufoula-Georgiou and two anonymous reviewers. Computer resources and precipitation data were provided by the Hydroscope Hydrometeorological Database System of the National Technical University of Athens.

References

- Bardossy, A., and E. Plate, Modelling daily rainfall using a semi-Markov representation of circulation pattern occurrence, *J. Hydrol.*, 122, 33-47, 1991.
- Bardossy, A., and E. Plate, Space-time model for daily rainfall using atmospheric circulation patterns, *Water Resour. Res.*, 28(5), 1247-1259, 1992.
- Baur, F., P. Hess, and H. Nagel, *Kalender der Grosswetterlagen Europas 1881-1939*, DWD, Bad Homburg, Germany, 1944.
- Dingman, L., *Physical Hydrology*, Prentice-Hall, Englewood Cliffs, N. J., 1994.
- Duckstein, L., A. Bardossy, and I. Bogardi, Linkage between the occurrence of daily atmospheric circulation patterns and floods: An Arizona case study, *J. Hydrol.*, 143, 413-428, 1993.
- Freund, J., and G. Simon, *Statistics, A First Course*, Prentice-Hall, Englewood Cliffs, N. J., 1991.
- Hay, L. E., G. J. McCabe Jr., D. M. Wolock, and M. A. Ayers, Simulation of precipitation by weather type analysis, *Water Resour. Res.*, 27(4), 493-501, 1991.
- Huff, F., Climatological assessment of natural precipitation characteristics for use in weather modification, *J. Appl. Meteorol.*, 8, 401-410, 1969.
- Hughes, J., and P. Guttorp, A class of stochastic models for relating synoptic atmospheric patterns to regional hydrologic phenomena, *Water Resour. Res.*, 30(5), 1535-1546, 1994.
- Joulis, V., Appraisal of space distribution of rainfall using Geographical Information Systems, Diploma thesis, Natl. Tech. Univ., Athens, 1996.
- Lamb, H. H., Types and spells of weather around the year in the British Isles, Annual trends, seasonal structure of the year, Singularities, *Q. J. R. Meteorol. Soc.*, 76, 393-438, 1950.
- Lamb, H. H., British Isles weather types and a register of the daily sequences of circulation patterns 1861-1971, 86 pp., *Geophys. Mem.* 116, 1972.
- Maheras, P., Synoptic Situations and Multidimensional Analysis of Weather in Thessaloniki, Monograph, Univ. of Athens, 1982.
- Mamassis, N., and D. Koutsoyiannis, Structure stochastique des pluies intenses par type de temps, *Publications de l'Association Internationale de Climatologie*, vol. 6, pp. 301-313, Thessaloniki, 1993.
- Mamassis, N., D. Koutsoyiannis, and I. Nalbantis, Intense rainfall and flood event classification by weather type, Presentation at the XIX EGS General Assembly, Grenoble (abstract), *Ann. Geophys.*, 12, Suppl. II, part II, C440, 1994.
- McCabe, G., A conceptual weather-type classification procedure for the Philadelphia, Pennsylvania area, *U.S. Geol. Surv. Water Resour. Invest. Rep.*, 89-4183, 1989.
- McCabe, G., Relationships between atmospheric circulation and snowpack in the Gunnison River basin, Colorado, *J. Hydrol.*, 157, 157-175, 1994.

- Schuepp, M., Kalender der Wetter und Witterungslagen von 1955 bis 1967, *Veröffentl. Schweiz. Meteorol. Zentralanst.*, 11, 1-43, 1968.
- Shaw, E., An analysis of the origins of precipitation in northern England, 1956-1960, *Q. J. R. Soc.*, 88, 539-547, 1962.
- Van de Gried, A., and E. Seyhan, Statistical analysis of weather-type runoff phenomena in an alpine environment, *J. Hydrol.*, 70, 51-69, 1984.
- Wilby, R., Stochastic weather type simulation for regional climate change impact assessment, *Water Resour. Res.*, 30(12), 3395-3403, 1994.
- Wilby, R., Simulation of precipitation by weather pattern and frontal analysis, *J. Hydrol.*, 173, 91-109, 1995.
- Wilby, R., B. Greenfield, and C. Glenn, A coupled synoptic-hydrological model for climate change impact, *J. Hydrol.*, 153, 265-290, 1994.
- Wilson, L., D. Lettenmaier, D., and E. Wood, Simulation of daily precipitation in the Pacific Northwest using a weather type classification scheme, *Surv. Geophys.*, 12(1-3), 127-142, 1991.

D. Koutsoyiannis and N. Mamassis, Department of Water Resources, Faculty of Civil Engineering, National Technical University, Heron Polytechniou 5, Zografou, GR-157 80, Greece. (e-mail: dk@hydro.civil.ntua.gr; nikos@hydro.civil.ntua.gr)

(Received October 27, 1995; revised April 15, 1996; accepted April 25, 1996.)

Copyright 1996 by the American Geophysical Union

Paper number 96JD01377.
0148-0227/96/96JD-01377\$09.00

Table 1. Summary Description of Weather Types

| Main Category | Abbreviation | Description of circulation |
|---|--------------|---|
| Continental anticyclones | A1 | location of center in western Europe or northern Atlantic |
| | A2 | location of center in Russian or Siberian region |
| | A3 | location of center in Balkan region |
| Maritime anticyclones | A4 | location of center in eastern Mediterranean |
| | A5 | location of center in western Mediterranean and northern Africa |
| Cyclones with zonal orbit | W1 | cyclone passes from the Balkans over 45° latitude |
| | W2 | cyclone passes through Greece below 45° latitude |
| Cyclones with meridional orbit | NW1 | cyclone originates from western Mediterranean or northwestern Europe and passes through Greece |
| | NW2 | cyclone circulates from Scandinavia to Black Sea |
| | SW1 | cyclone passes to the west of the line Malta - western Macedonia - Ukraine |
| | SW2 | cyclone passes to the east of the line Malta - western Macedonia - Ukraine |
| Mixed types | MT1 | presence of an anticyclone over the central-northern Europe and a cyclone over Black sea; isobars at surface have meridional arrangement |
| | MT2 | presence of an anticyclone over the central - northern Europe and a cyclone over eastern Mediterranean or Aegean sea; isobars in surface have no specific arrangement |
| Characteristic types (special, mostly dry period types) | DES | special combination between low pressure in southeastern Asia and very weak gradient in Balkans (dry type) |
| | MB | very weak pressure gradient over Greece |
| | DOR | presence of a cold air mass at the 500-hPa level above Greece |

Table 2. Probability of Occurrence of Intense Point Rainfall Events, Conditional on the Prevailing Weather Type

| Weather Type | Rainy Season | | | Dry Season | | |
|--------------|----------------------|---------------------------------|------------------------------|----------------------|---------------------------------|------------------------------|
| | Total Number of Days | Number of Intense Rainfall Days | Probability of Occurrence, % | Total Number of Days | Number of Intense Rainfall Days | Probability of Occurrence, % |
| A1 | 346 | 1 | 0.3 | 237 | 0 | 0.0 |
| A2 | 372 | 1 | 0.3 | 268 | 0 | 0.0 |
| A3 | 199 | 0 | 0.0 | 161 | 0 | 0.0 |
| A4 | 146 | 0 | 0.0 | 67 | 0 | 0.0 |
| A5 | 101 | 0 | 0.0 | 13 | 0 | 0.0 |
| W1 | 155 | 15 | 9.7 | 155 | 4 | 2.6 |
| W2 | 123 | 17 | 13.8 | 4 | 1 | 25.0 |
| NW1 | 571 | 63 | 11.0 | 36 | 4 | 11.1 |
| NW2 | 266 | 14 | 5.3 | 268 | 9 | 3.4 |
| SW1 | 615 | 71 | 11.5 | 238 | 14 | 5.9 |
| SW2 | 215 | 14 | 6.5 | 48 | 2 | 4.2 |
| MT1 | 149 | 0 | 0.0 | 91 | 4 | 4.4 |
| MT2 | 278 | 0 | 0.0 | 4 | 0 | 0.0 |
| DES | 0 | 0 | - | 317 | 7 | 2.2 |
| MB | 577 | 1 | 0.2 | 801 | 21 | 2.6 |
| DOR | 132 | 3 | 2.3 | 352 | 27 | 7.7 |
| Total | 4245 | 200 | | 3060 | 93 | |

Table 3. Statistics of Hourly Depth

| Rainy Period | | | | Dry Period | | | |
|--------------|----------------|------------------------|------------------------|--------------|----------------|------------------------|------------------------|
| Weather Type | Mean Value, mm | Standard Deviation, mm | Lag 1 Auto-correlation | Weather Type | Mean Value, mm | Standard Deviation, mm | Lag 1 Auto-correlation |
| SW1 | 1.8 | 2.6 | 0.55 | SW1,SW2, | | | |
| SW2 | 1.2 | 1.9 | 0.54 | W1, W2 | 2.0 | 3.7 | 0.44 |
| NW1 | 1.6 | 2.2 | 0.55 | NW1,NW2 | 3.6 | 6.1 | 0.20 |
| NW2 | 2.0 | 2.6 | 0.58 | DOR | 3.2 | 5.5 | -0.03 |
| W1 | 1.5 | 2.0 | 0.38 | Rest | 3.4 | 4.9 | 0.01 |
| W2 | 2.0 | 3.5 | 0.56 | | | | |

Table 4. Percentage of Variance in Point Intense Rainfall Characteristics Explained by Weather Types

| Variable | Rainy Season | Dry Season |
|----------------|--------------|------------|
| Duration | 7% | 18% |
| Total depth | 3% | 18% |
| Mean intensity | 7% | 8% |
| Hourly depth | 1% | 2% |

Table 5. Mean Daily Depth of Intense Rainfall Days (mm) for Each Subarea and Each Weather Type

| Subarea | Weather Type | | | | | | | |
|-------------------|--------------|------|------|------|------|------|-------|------|
| | W1 | W2 | SW1 | SW2 | NW1 | NW2 | MT1,2 | Rest |
| Leftkada | 13.9 | 21.2 | 22.6 | 8.7 | 16.9 | 12.3 | 2.1 | 2.6 |
| Upper Acheloos | 16.4 | 23.1 | 24.0 | 7.5 | 16.9 | 14.0 | 2.2 | 3.2 |
| Lower Acheloos | 32.8 | 29.8 | 33.7 | 13.4 | 25.9 | 13.8 | 5.3 | 3.2 |
| Mornos-Evinos | 25.1 | 27.6 | 25.5 | 13.7 | 22.8 | 17.6 | 5.4 | 5.9 |
| Sperchios | 12.2 | 15.6 | 15.2 | 19.5 | 19.7 | 6.7 | 14.6 | 4.6 |
| Biotikos Kifissos | 4.2 | 8.4 | 7.4 | 19.7 | 14.9 | 4.0 | 18.2 | 2.9 |
| Assopos | 0.9 | 4.3 | 3.6 | 15.9 | 9.4 | 2.1 | 13.9 | 0.5 |
| Athens | 0.6 | 3.6 | 3.9 | 15.5 | 9.4 | 1.5 | 12.0 | 0.3 |
| Evia | 0.7 | 4.1 | 3.7 | 25.0 | 12.4 | 3.3 | 36.5 | 0.9 |
| Skyros | 0.6 | 9.1 | 2.7 | 9.1 | 7.2 | 4.3 | 7.0 | 0.8 |
| Total area | 12.4 | 15.3 | 15.5 | 16.4 | 17.0 | 8.1 | 13.8 | 2.6 |
| Number of events | 18 | 23 | 88 | 28 | 96 | 10 | 41 | 12 |

Table 6. Percentage of Variance of Areal Daily Intense Rainfall Explained by Weather Types

| Subarea | Percentage, % | Subarea | Percentage, % |
|----------------|---------------|-------------|---------------|
| Leftkada | 24.8 | B. Kifissos | 21.8 |
| Lower Acheloos | 27.3 | Assopos | 24.9 |
| Upper Acheloos | 26.5 | Athens | 14.7 |
| Mornos-Evinos | 25.5 | Evia | 47.4 |
| Sperchios | 10.2 | Skyros | 6.3 |

Figure Captions

Figure 1. Study area: (a) morphology, (b) separated subareas and rain gages (with the Krikello rainrecorder being the triangle), (c) general location.

Figure 2. Main trajectories of cyclonic weather types.

Figure 3. Map of the 500 hPa level of the event of July 7, 1970 06 00 UT.

Figure 4. Probability of occurrence of intense rainfall events per group of weather types: (a) Groups of rainy period (A: W1, W2, NW1, SW1; B: SW2, NW2; C: MT2, DOR; D: A1-A5, MT1, DES, MB); (b) Groups of dry season (A: W2, NW1, DOR; B: SW1, SW2; C: W1, NW2, MT1, DES, MB; D: A1-A5, MT2).

Figure 5. Box plots of rainfall event characteristics at Krikello: (a) duration, (b) total depth, and (c) mean intensity. The middle line of each box represents the median, the bottom and top lines represent the lower and the upper quartile, and the whiskers represent the minimum and maximum observed values.

Figure 6. Statistical surfaces of weather types. First column, mean (mm); second column, standard deviation (mm); third column, coefficient of variation.

Figure 7. Box plots of computed correlation coefficients between rainfall fields per weather type. The middle line of each box represents the median, the bottom and top lines represent the lower and the upper quartile, and the whiskers represent the minimum and maximum observed values.

Figure 1. Study area: (a) morphology, (b) separated subareas and rain gages (with the Krikello rainrecorder being the triangle), (c) general location.

Figure 2. Main trajectories of cyclonic weather types.

Figure 3. Map of the 500 hPa level of the event of July 7, 1970 06 00 UT.

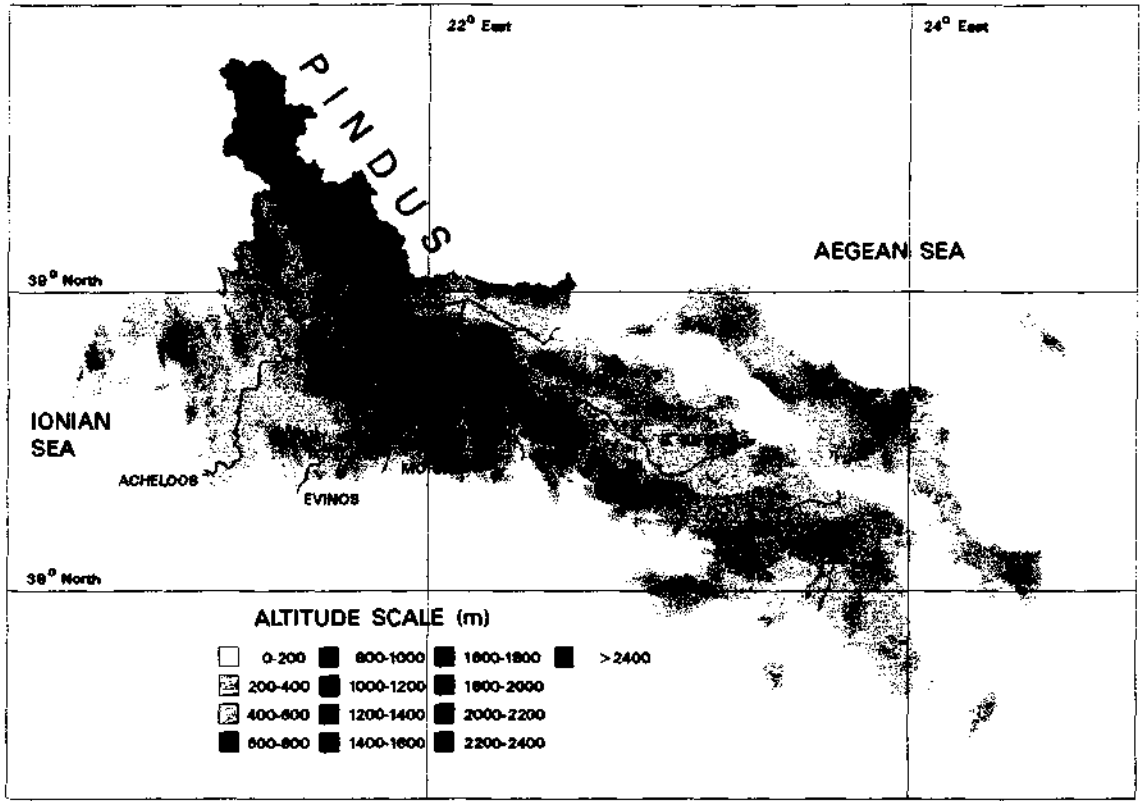
Figure 4. Probability of occurrence of intense rainfall events per group of weather types: (a) Groups of rainy period (A: W1, W2, NW1, SW1; B: SW2, NW2; C: MT2, DOR; D: A1-A5, MT1, DES, MB); (b) Groups of dry season (A: W2, NW1, DOR; B: SW1, SW2; C: W1, NW2, MT1, DES, MB; D: A1-A5, MT2).

Figure 5. Box plots of rainfall event characteristics at Krikello: (a) duration, (b) total depth, and (c) mean intensity. The middle line of each box represents the median, the bottom and top lines represent the lower and the upper quartile, and the whiskers represent the minimum and maximum observed values.

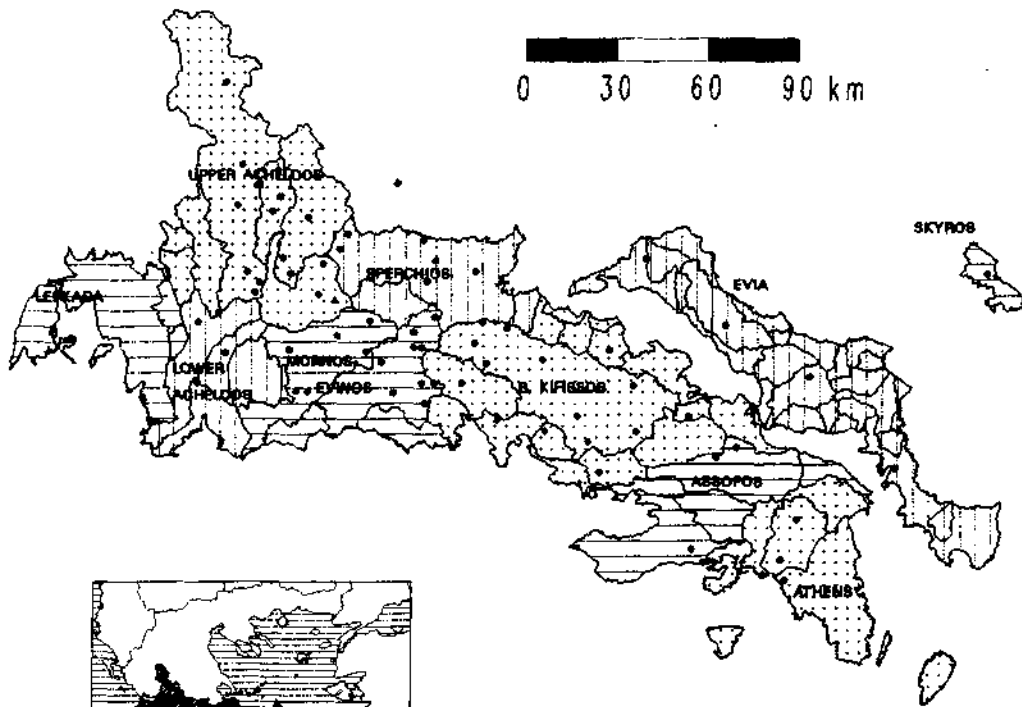
Figure 6. Statistical surfaces of weather types. First column, mean (mm); second column, standard deviation (mm); third column, coefficient of variation.

Figure 7. Box plots of computed correlation coefficients between rainfall fields per weather type. The middle line of each box represents the median, the bottom and top lines represent the lower and the upper quartile, and the whiskers represent the minimum and maximum observed values.

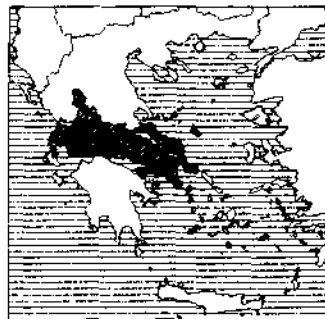
(a)



(b)



(c)



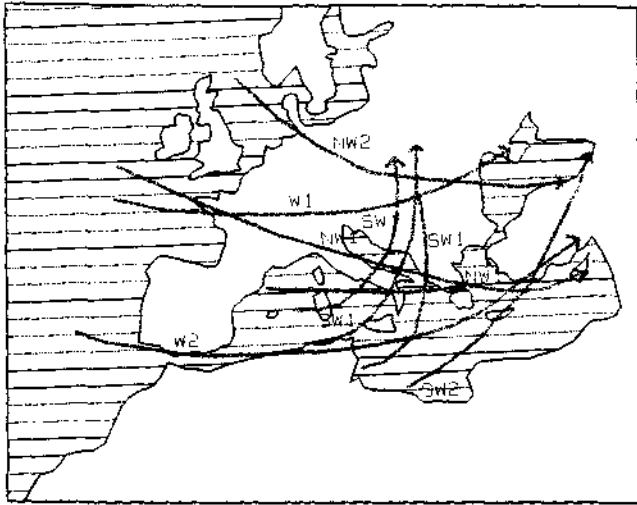


Figure 2

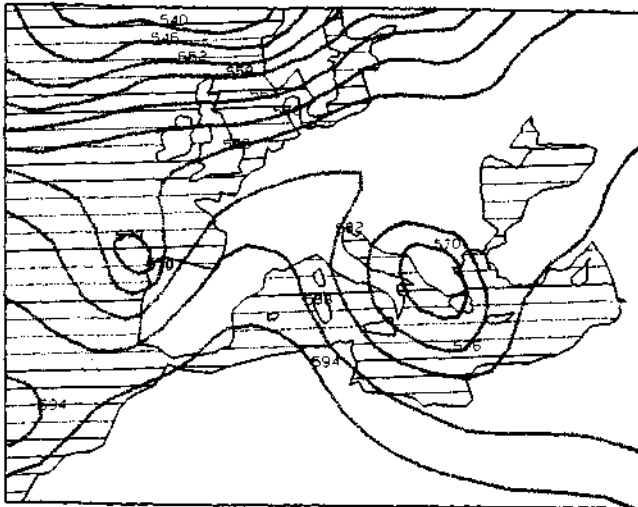


Figure 3

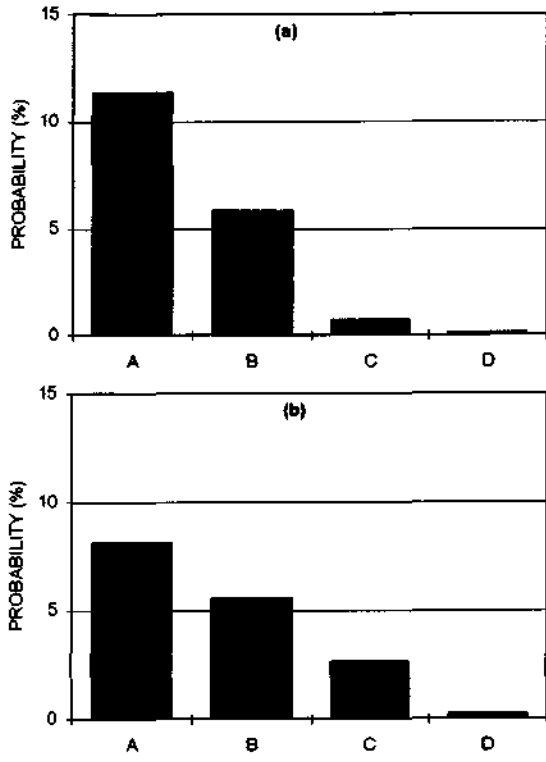


Figure 4

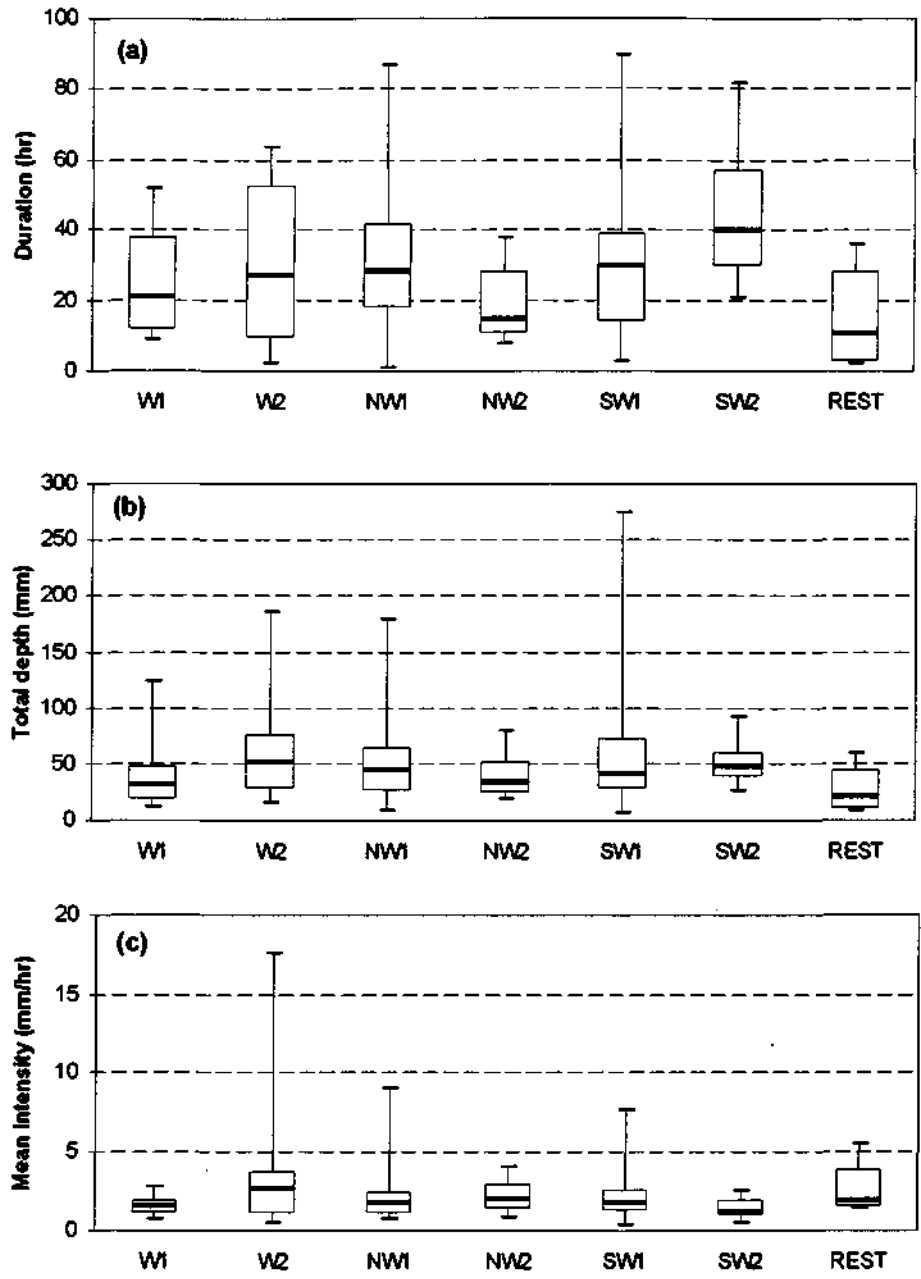
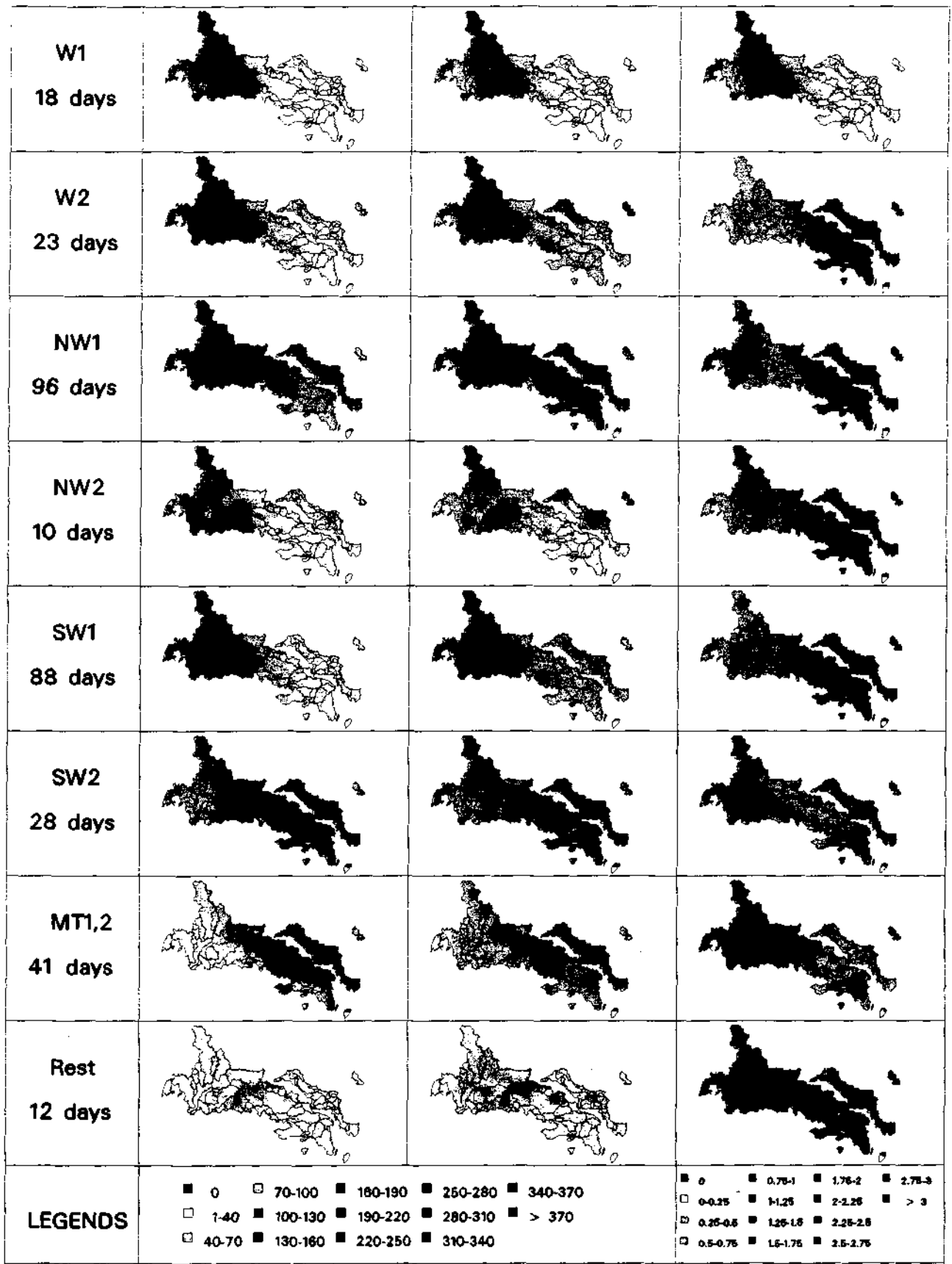


Figure 5
Please reduce it



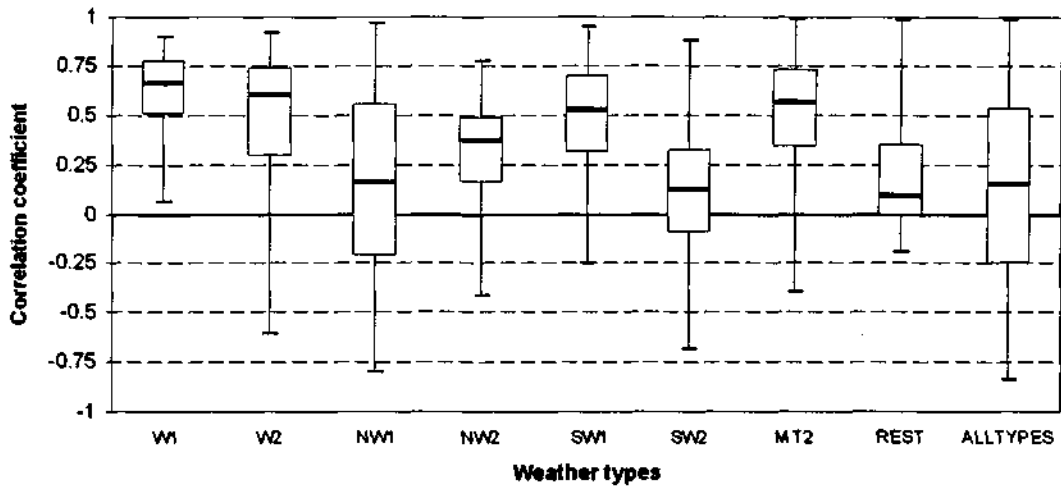


Figure 7
Please reduce it